TIME DEPENDENT HEAT TRANSFER RATES IN HIGH REYNOLDS NUMBER HYPERSONIC FLOWFIELDS

Michael J. Flanagan
The Aeronautical and Astronautical Research Laboratory
The Ohio State University
Columbus, OH

ABSTRACT

Time dependent heat transfer rates have been calculated from time dependent temperature measurements in the vicinity of shock-wave boundary-layer interactions due to conical compression ramps on an axisymmetric body. The basic model is a cylindrical body with a 10° conical nose. Four conical ramps, 20°, 25°, 30°, and 35° serve as shock wave generators. Flowfield surveys have been made in the vicinity of the conical ramp vertex, the separation point, and the reattachment point. A significant effort was made to characterize the natural frequencies and relative powers of the resulting fluctuations in heat transfer rates. This research effort, sponsored jointly by NASA and the Air Force, was conducted in the Air Force Flight Dynamics Directorate High Reynolds Facility. The nominal freestream Mach number was 6, and the freestream Reynolds numbers ranged from 2.2 Million/ft to 30.0 Million/ft.

Experimental results quantify temperature response and the resulting heat transfer rates as a function of ramp angle and Reynolds number. The temperature response within the flowfield appears to be steady-state for all compression ramp angles and all Reynolds numbers, and hence, the heat transfer rates appear to be steady-state.

INTRODUCTION

Highlighted by the well-documented in-flight failure of an external support strut on the X-15 flight test vehicle, the problem of shock-wave boundary-layer interactions in hypersonic flowfields has been of interest for almost five decades. In contrast to the so-

called "free-interaction" problem where the impinging shock provides the mechanism for the induced separation, this study is concerned with the separation induced by means of a compression ramp. The resulting interaction between the shock system affects the local flowfield in the interaction region as well as reattachment of the flowfield downstream of the ramp vertex and, hence, seriously effects the overall flowfield structure. With the added intensity of the severe temperature gradients and thin boundary layers that exist at hypersonic flight conditions, an environment is created that is capable of destroying many known materials. The requirements needed to cope with these intense flowfields is currently influencing configuration development as well as defining the focus of basic research efforts in present day aerodynamics.

A region on a hypersonic vehicle that would be particularly vulnerable to dynamic heating due to shock-wave boundary-layer interactions is near control surface hinge points. As the ability to achieve sustained hypersonic flight becomes a reality, the need for maneuverability and acceptable control loads becomes essential. The effects of high-temperature flowfield dynamics within the separated regions caused by the deflection of these control surfaces needs to be understood before any credible system can be designed.

This experimental study investigates the heat transfer rates in the vicinity of a conical ramp in a turbulent, hypersonic flowfield. The results characterize the magnitude, dynamic nature, and characteristic frequencies of the fluctuation levels.

MODEL DESCRIPTION

Conducted in the Air Force Flight Dynamics Directorate (WL) High Reynolds Facility (HRF) over a period of some four weeks, this test was provided to The Ohio State University (OSU) through a Cooperative Testing Agreement with WL. This Mach 6 facility is capable of producing Reynolds numbers ranging from approximately 2.0×10^6 per foot to a maximum as high as 30.0×10^6 per ft.

The HRF wind tunnel model is shown in Figure 1. Fabricated from 17-4 PH stainless steel, the model is a cylindrical body 1.558 inches in diameter and 15.1 inches in length. The nose is a 10° cone. Four conical ramps of angles 20°, 25°, 30°, and 35° are provided to

act as shock generators. These ramps can be positioned along the body surface from fuselage station (FS) 10.80 , referenced from the nose (FS = 0.0), as far aft to FS 14.85.

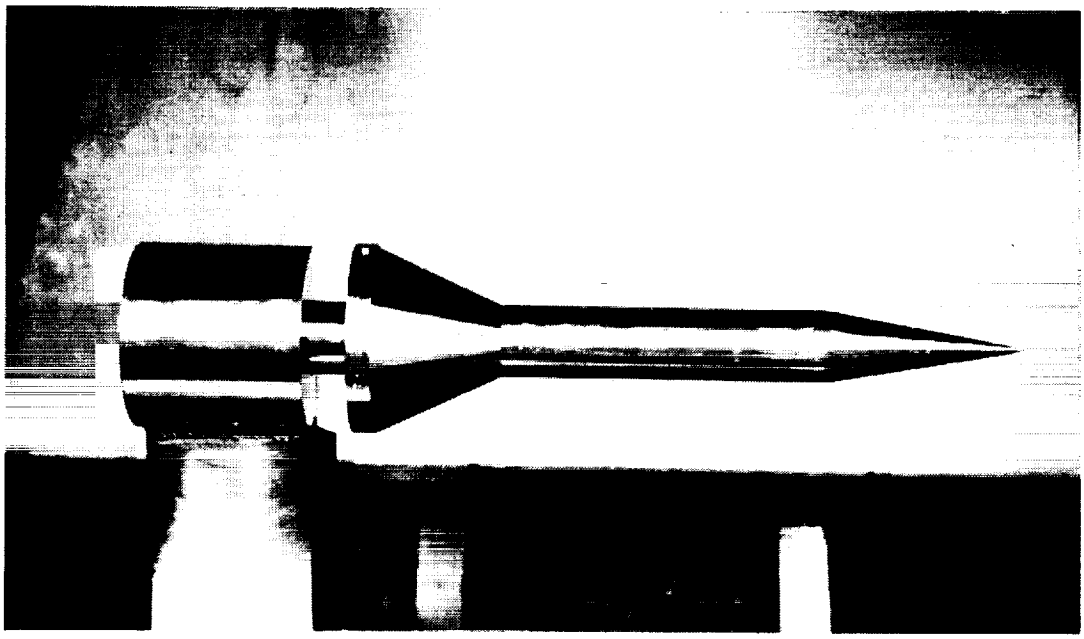

Figure 1. HRF axisymmetric model description

Four coaxial thermocouple gauges are located in a dedicated instrumentation section. These gauges are mounted within the model wall at FS 10.15, 10.35, 10.55, and, 10.75. Additionally, two pressure transducers are mounted within this instrumentation section at FS 10.35 and 10.75 for the simultaneous measurement of pressure fluctuation characteristics. This gauge distribution provides the most economical compromise between data resolution quality (measurement interval along the body) and test time requirements (the number of ramp translation points). This arrangement allows a comprehensive survey of the separation and reattachment regions with the least number of ramp location changes.

Simultaneous measurement of the temperature and pressure data will allow correlations between the characteristic frequencies within the flowfield environment. Once correlated with the pressure data, the frequencies of these temperature data acquired during the test in the HRF can be compared to previous works highlighting shock-wave boundary-layer interactions wherein only pressure data are currently available.

Figure 2 provides a graphic representation of the intensity of the temperatures typical of the test environment for this research work. This figure shows the temperature time-history at a point on the model surface during a typical data run in the Air Force Flight Directorate High Reynolds Facility (HRF). Any sensing device used in this environment must be capable of extreme sensitivity in order to detect fluctuations on the order of several percent of the freestream level and still withstand the peak heating rates encountered within the free-jet.

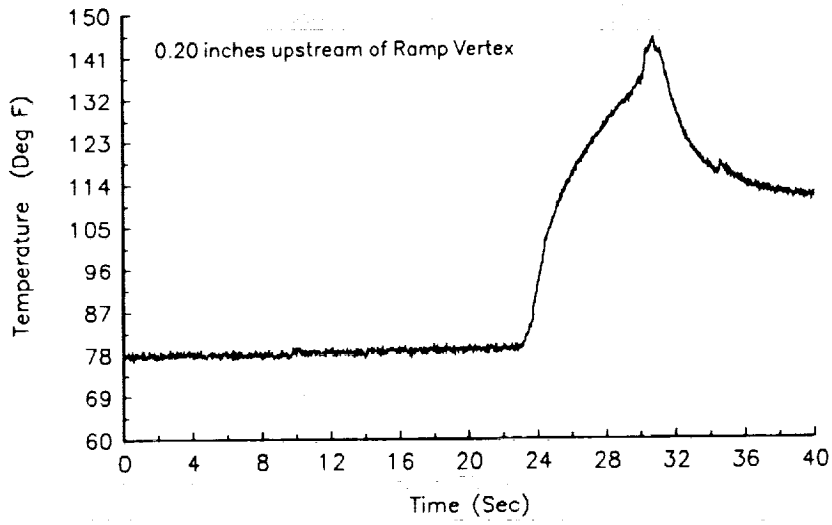

Figure 2. Typical HRF temperature environment : Re_∞ = 30 M/Ft

Supporting the concerns for gauge selection and survivability issues, References 1 and 2 address the acquisition of time dependent data in a dynamic testing environment. These papers discuss key issues for reliable data acquisition in fluctuating flowfields. With the intense heating rates that exist in hypersonic, high Reynolds number flowfields, these studies combine to suggest a common theme for instrumentation selection. Specifically, the selection of these gauges should be based upon gauge survivability. High frequency response should not be the only primary consideration.

The primary instrumentation for this study is the coaxial thermocouple gauge. Shown in Figure 3, these coaxial gauges can withstand temperatures in excess of 2000° R while still having a dynamic response in excess of 50 kHz. These gauges, described in Reference 3, are more robust than thin-film types, described in Reference 4, and do not introduce the uncertainty of thermal disturbances within the flowfield due to dissimilar thermal properties between the model body and the gauge material or substrate.

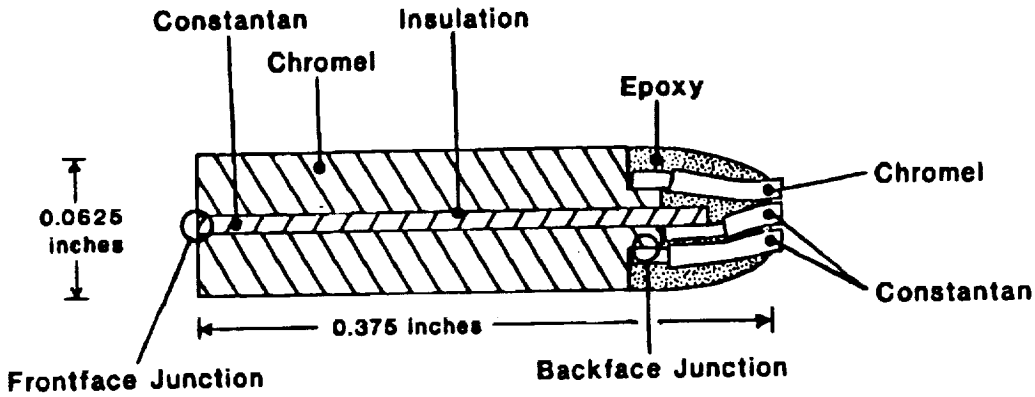

Figure 3. Coaxial thermocouple gauge description

The thermocouple junction is created when, by sanding with 180 grit paper, chromel and constantan slivers are blended in the infinitesimally small region over the insulation separating the two dissimilar metals. The resulting sensing surface resembles an annular ring with dimensions of approximately 0.016 inches for the overall annular ring diameter and approximately 0.0005 inches for the width of the actual sensing ring diameter. This remarkably small size, and hence thermal mass, is the reason for the capability to respond to high-frequency temperature fluctuations.

A preliminary model was constructed as a test-bed for verification of the coaxial gauge response characteristics. This model has a cylindrical body of two-inch length with a hemispherical nose of one inch diameter. The model was sting mounted with one coaxial

thermocouple gauge installed at the nose stagnation point. Experimental data was taken during runs in the OSU 12-inch hypersonic tunnel at Mach numbers of 6, 10, and 12. Comparison runs were made in the WL 20-inch hypersonic tunnel at Mach 12. Figure 4 presents typical test data from the OSU AARL facility. Notice the time delay in response between the front and rear thermocouple junctions.

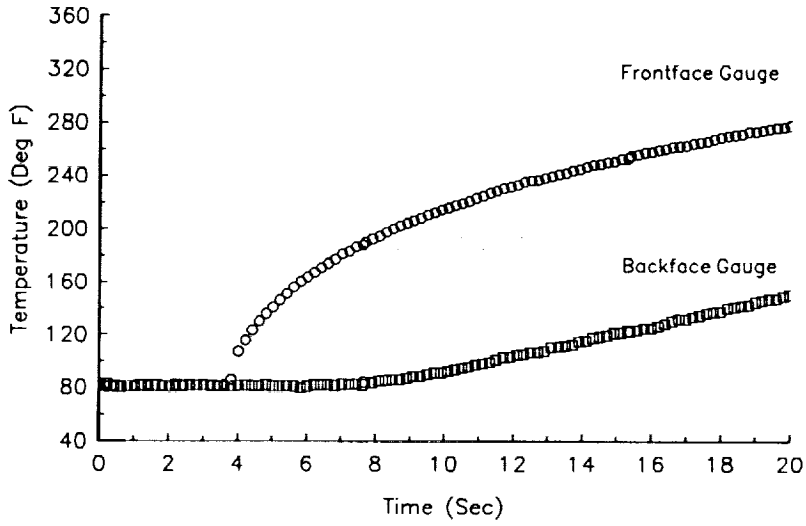

Figure 4. Typical coaxial thermocouple gauge temperature response

The theoretical time-delay in temperature response between the front and rear surface junctions is determined from the thermal characteristics of the gauge material. For purely one-dimensional heat transfer, the time increment for a heat pulse to travel the length of the gauge from the front surface junction to the back surface junction is given by the equation

$$t_D = \frac{0.2L^2}{\alpha} \qquad (1)$$

where α is the thermal diffusivity for a gauge of length (L).

Now for a gauge length of 0.375 inches, this theoretical time delay is approximately 3.7 seconds. Since Figure 4 shows a time delay of approximately 1.7 seconds, it can be

presumed that the heat transfer is not locally one-dimensional. In fact, close inspection of the model reveals that the gauge length is of the same order of magnitude as the model characteristic length, the nose diameter.

Figure 5 shows a comparison between the steady-state heating rates on this model from the two facilities. These heat transfer results are based upon a one-dimensional, semi-infinite slab thermal model. This data reduction method is not consistent with the model design for infinite time as shown in Figure 4; however, for the first few moments, the assumptions should be sufficient for assessing basic, steady-state gauge performance. As the data is valid for approximately the first two seconds of test data, the initial heating gradients and the peak heating rates should be accurate enough for this preliminary gauge evaluation.

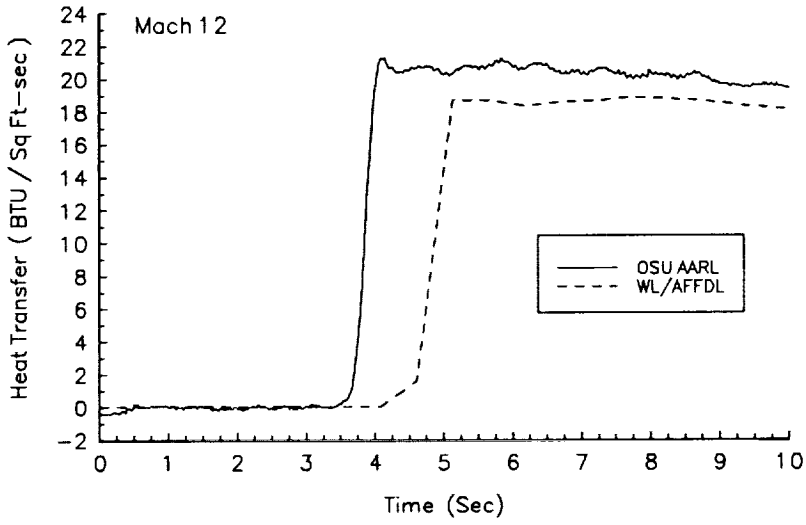

Figure 5. Comparison of stagnation point heating rates

Additional tests were performed to assess the effect of the gauge installation on the output voltage. Figure 6 shows a comparison between voltage output for a freestanding gauge and a gauge mounted within the test-bed model. The model material is 17-4 PH stainless steel. Both gauge arrangements were simultaneously exposed to the same oil bath. The temperature response was recorded. From these data it can be seen that any secondary voltage created from the gauge/model-material interface is insignificant.

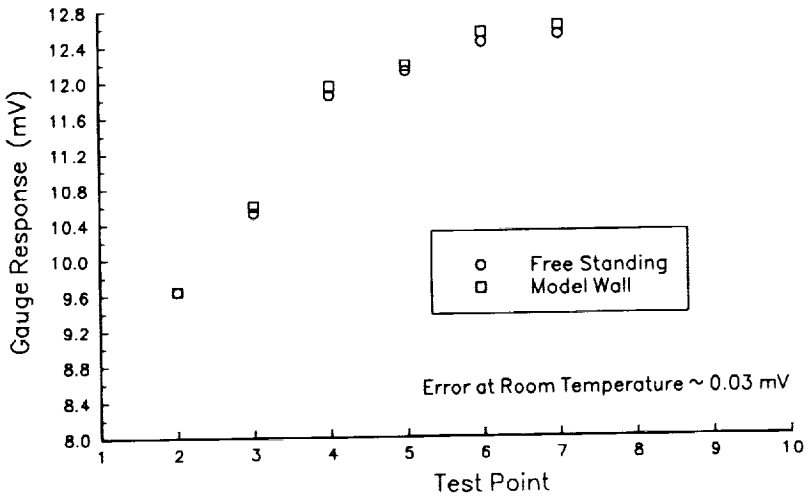

Figure 6. Effect of secondary thermocouple junction on gauge output

The coaxial gauge manufacturer, Medtherm Corp, quotes response times ranging from 100 kHz to 1 MHz depending upon the thermocouple junction treatment (sanded or coated); however, no documentation was made available to the author. Some means to test the high-frequency response characteristics of this gauge design was necessary. With the invaluable assistance of Mr. Greg Elliot, a PhD candidate in at OSU, a temporary test facility was constructed with components adapted from a laser doppler velocimetry (LDV) system at the OSU Aeronautical and Astronautical Research Lab (AARL).

The frequency response of the gauge was tested using a system comprised of a low power (1-watt) laser and a high-frequency chopper. The coaxial gauge, installed in the instrumentation section of the HRF model, was pulsed at frequencies of 20, 40, and 80 kHz. The data was recorded by both the high-speed data acquisition system at AARL and a real-time fast-fourier transformation (FFT) analyzer. The data were reduced to temperature traces and then analyzed both on-line and off-line for frequency content. Figure 7 shows the basic temperature response of the gauge at a pulse rate of 20 kHz. Notice the sinusoidal nature of the test data. The corresponding power spectrum of this data is presented in Figure 8. Notice the dominant peak of energy at 20 kHz. Similar results were obtained at the 40 kHz and 80 kHz pulse rates.

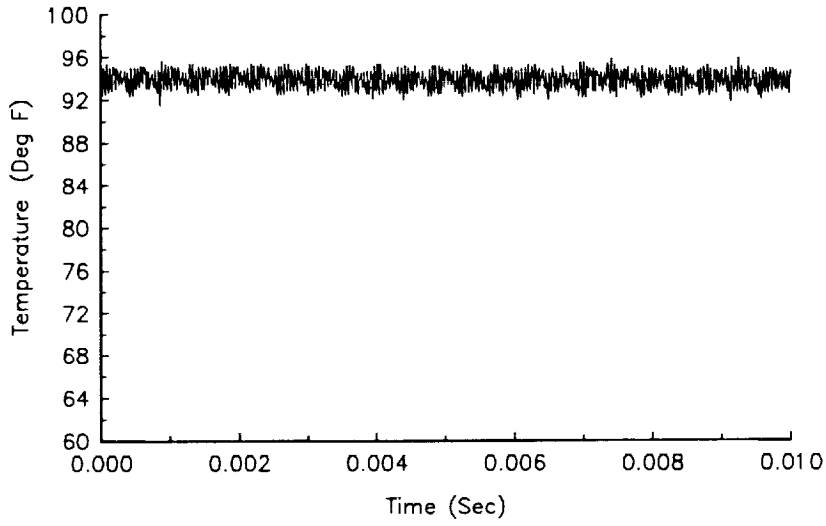

Figure 7. Coaxial gauge response: laser diagnostics at 20 kHz

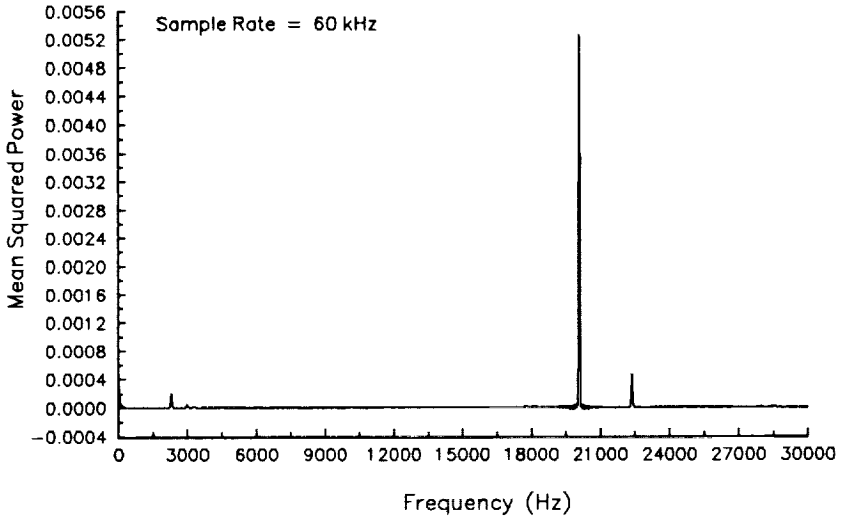

Figure 8. PSD for gauge laser diagnostics: pulse rate at 20 kHz

Based upon the results of these initial laser diagnostic tests, combined with simple bench tests and the gauge/model-material interface analysis, a confidence level was reached wherein it was believed that the coaxial thermocouple gauges would perform as advertized.

DATA ACQUISITION

For the test in the HRF, the data acquisition system, described in Reference 5, was a 12-bit, 16-channel sample-and-hold and A/D board that was combined with a 25 mHz, Intel 386-based personal computer. This system was created by AARL personnel in order to provide portable, unsteady-data acquisition capability at a remote test facility that did not have that capability.

The data acquisition system was configured with stand-alone filter and signal conditioning equipment that amplified and filtered the signals from the instrumentation prior to sampling by the A/D board. The signal conditioning equipment and the filter units were installed just outside of the tunnel test section. As a result, the amplified and filtered signal could then be sent through shielded cables to the data acquisition computer, located approximately 50 feet from the test section, with less concern for electrical noise[5].

DATA REDUCTION

After the acquired temperature data traces are examined, the data are reduced to time dependent heat transfer rates. Spectral analysis is then performed to determine the characteristic frequencies and corresponding power levels of the fluctuations. The heat transfer calculations are based upon the methods presented in References 6 and 7. These methods are currently in use at WL and are the basis for most heat transfer analysis in the Flight Mechanics Group (FLMG). These numerical analysis methods are generally based upon the assumption of 1-D or 2-D conduction paths for boundary conditions that are representative of either infinite, semi-infinite, or finite slab approximations. As the exact characteristics of the heat transfer paths are unknown, evaluation of the model geometry and gauge installation is essential for proper choice of the numerical scheme.

For the axisymmetric HRF model used for this research work, the gauges are located along the body surface. The gauge length is 0.375 inches and the wall thickness is approximately 0.40 inches. The instrumentation section is approximately 11 inches from the nose region and the axisymmetric flowfield should be well established. As the gauge length is of the order of one-fifth of the body diameter, the body is of a homogenous construction of a material with thermal properties close to those of the gauge material, and, as the test times are of the order of 1 second, the assumption that the thermal path could be approximated by one-dimensional conduction into a semi-infinite solid is appropriate.

The relationship between surface temperature and one-dimensional heat conduction into a homogenous semi-infinite solid is given by the equation

$$\dot{q}(t) = \sqrt{\frac{\rho c k}{\pi}} \int_0^t \frac{dT(\tau)}{d\tau} \frac{d\tau}{\sqrt{t-\tau}} \qquad (2)$$

where, ρ, c, and k are respectively the gauge material density, specific heat, and thermal conductivity.

This method, called the direct method, can be used directly on the test data. However, the finite difference scheme is very sensitive to noise in the test data. As this methodology will be applied to high-frequency data, it is possible that the fluctuating components could have the same affect on the numerical scheme as noise. An alternate scheme, referred to as the indirect method, calculates the cumulative heat pulse Q(t) and then differentiates that pulse with time to obtain q(t). The initial calculations for Q(t) tend to smooth the data and produce a method less sensitive to data noise. This heat pulse, Q(t), is calculated from the following equation

$$Q(t) = \sqrt{\frac{\rho c k}{\pi}} \int_0^t \frac{T(\tau)}{\sqrt{t-\tau}} \, d(\tau) \qquad (3)$$

and in finite difference form,

$$Q_n = \sqrt{\frac{\rho c k}{\pi}} \sum_{j=1}^{n} \frac{(T_j + T_{j-1})\,(t_n t_{n-1})}{\sqrt{t_n - t_j} - \sqrt{t_n - t_{j-1}}} \quad . \qquad (4)$$

This indirect method provides a more computationally-stable method for calculating the heat transfer rates. However, the intent of this research effort is to detect and analyze the

unsteady nature of the temperature fluctuations. Whether or not the effect of this "smoothing" of the data by this indirect method is significant, specifically, whether or not the indirect method removes any of the measured frequency content, will need to be investigated.

Since the heat conduction can be determined from integration of the heat pulse function Q(t), q(t) can be computed from the following equation:

$$\dot{q}_n = \left(\frac{1}{40\,(t_n - t_{n-1})}\right)\left[-2Q_{n-8} - Q_{n-4} + Q_{n+4} + 2Q_{n+8}\right] \quad . \qquad (5)$$

Calculation of the frequency content of the temperature data is accomplished through spectral analysis. Dozens of methods for spectral analysis exist; however, most techniques refer to the methodology proposed by Blackmann and Tukey in Reference 8. Reference 9 is strongly based on the works of Blackmann and Tukey, and forms the basis for the chosen method of data reduction. The details for the mathematical scheme used for this analysis can be found in Reference 10. Generally, frequency content is presented by means of a power spectral density (PSD) plot of energy (in dB) versus frequency. As there is no known means of presenting the energy content of temperature fluctuations in terms of decibels, the spectral analysis methodology chosen for this analysis was selected because the final product is linear with frequency.

EXPERIMENTAL RESULTS

Initial flowfield data, functions of ramp angle and body Reynolds number, Re_b, were comprised of schlieren photographs. Studies of these photographs determined the most likely locations of flowfield separation and reattachment as a function of distance from the fixed ramp vertex. Initial ramp locations, determined from these photo surveys, were chosen in an attempt to locate the estimated separation point in the center of the instrumentation section. Following runs would survey both upstream and downstream of this fuselage station in increments of 0.05 inches in an attempt to locate the region of peak temperature and pressure fluctuations. Once the peak location was determined, this separation point was surveyed extensively at different sampling rates and filter settings in an attempt to characterize the nature of the fluctuations.

Figure 9 is an example of a typical turbulent interaction, at a Re_b = 21.66 M, and shows the size of the interaction region relative to the body diameter of 1.55 inches. This turbulent-type of interaction is characterized not only by a very small separation bubble, generally on order of the boundary layer thickness (δ), but also by a very large separation angle, generally very close in value to that of the conical shock angle.

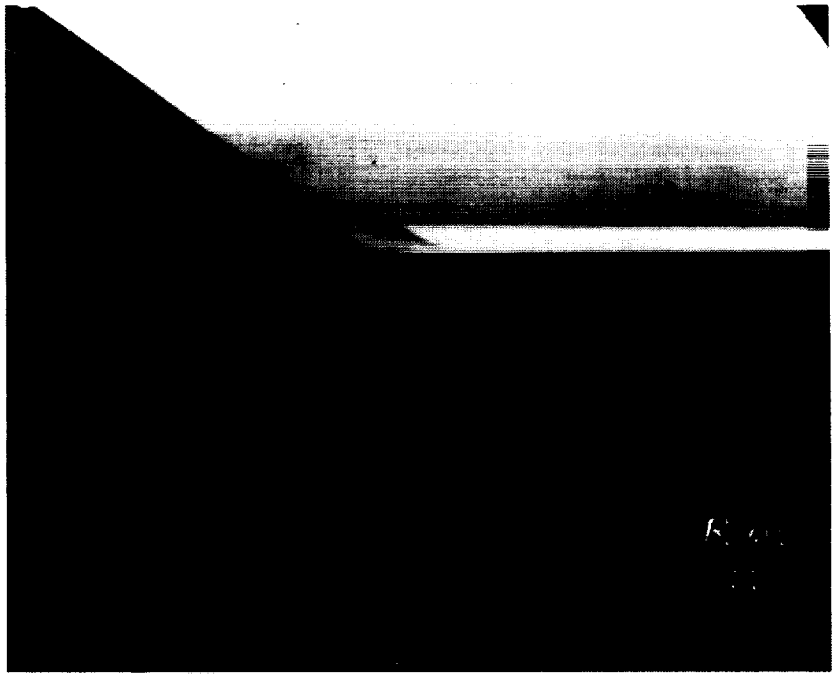

Figure 9. Schlieren photograph of a typical turbulent interaction

Analysis of the schlieren photographs during the HRF test showed variations of separation bubble size with ramp angle and Reynolds number. Post run analysis of the 35° ramp showed the separation bubble, at Re_b = 21.66 M, to be of the order of 10δ. The resulting reattachment point was located approximately 7δ along the ramp surface downstream from the vertex. As the 35° ramp is approximately 0.4 inches deep at this point, it was possible to mount eight coaxial thermocouple gauges along the ramp surface in an attempt to locate the reattachment point and to characterize the nature of any temperature fluctuations in that vicinity as well.

The temperature data were examined for trends and characteristics indicating some type of flowfield dynamics. Each data trace was further reduced through spectral analysis

techniques and examined for frequency content and the relative power contained in the data signal. Figure 10 shows typical temperature traces for the type of interaction presented in Figure 9. These traces represent temperature time-histories for three body locations in the vicinity of the separation point due to the 30° ramp. These data exhibit similar characteristics upstream, downstream, and in the vicinity of the separation point.

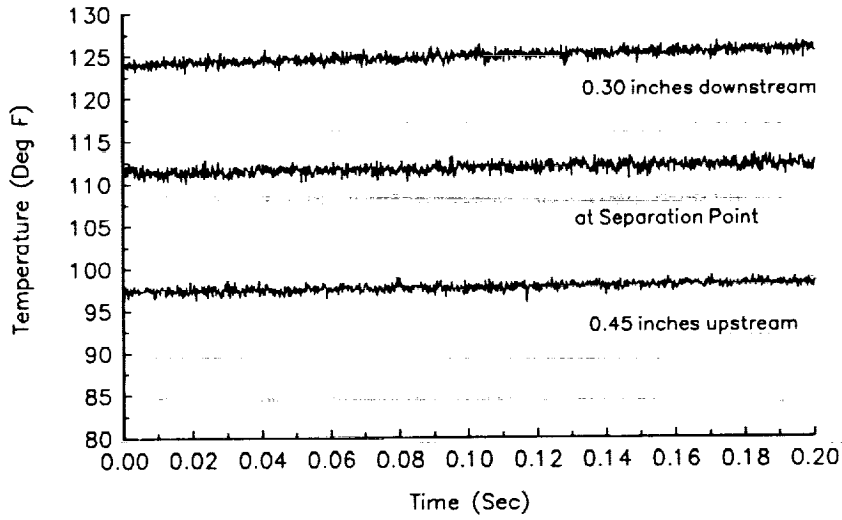

Figure 10. Typical Temperature Response: 30° Ramp at Re_b = 21.66 M

These data show some unsteadiness in temperature response. However, the RMS values are of insignificant magnitude. The magnitude of these fluctuations are approximately 0.5° F in the vicinity of the separation point and approximately 1.0°F in the vicinity of the reattachment point. Comparison of these data to the initial flowfield surveys of the HRF facility shows the ratio of these RMS values to the freestream temperature fluctuation levels to be of the order unity. The absence of any significant time-dependent components in this data, combined with the fact that these trends are repeated for 12 Reynolds numbers ranging from 1.62 to 21.66 M/ft and the ramp angles ranging from 20° to 35°, strongly suggests that the temperature response, and hence, the heat transfer rates, in these interacting regions are steady-state. Furthermore, these same trends were repeated for the data recorded at the reattachment point on the 35° ramp. Although the heating rate at the reattachment point was of the order of 600° F per minute, the temperature response also appears to be steady-state.

Figure 11 presents the results of calculations for the steady-state heat transfer in the vicinity of the separation point on the 30° ramp at Re_b = 21.66 M. These data show an average heat transfer rate of approximately 5.0 BTU/Ft^2-sec for the two body locations upstream of the separation point and approximately 9.0 BTU/Ft^2 -sec downstream of the separation point. The peak heating spike in the data at approximately 6 seconds is the result of the model insertion through the open-jet wake. Notice the heating rate downstream of the separation point, in the subsonic interaction region, is almost twice the level upstream.

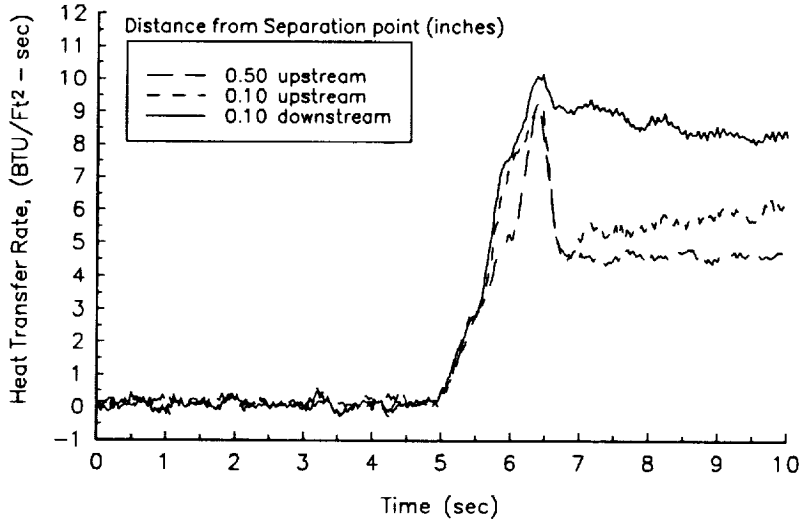

Figure 11. Heating Rate Near Separation: 30° Ramp, Re_b= 21.66 M

Figure 12, in contrast, presents heat transfer data within a laminar-type interaction region for the same model configuration at Re_b = 4.33 M. The term "laminar-type" refers to the shallow interaction angle and large separation bubble as shown in Figure 13. Consider that all of the data from Figure 12 is within the separation bubble. If we take this value to be approximately twice that of the upstream heating levels, as seen in the data trends from Figure 11, the upstream heating rate for this interaction at 4.33 M can be approximated at 0.75 BTU/Ft^2-sec. This value is of the order of one-eighth the heating rate for the same configuration at Re_b 21.66 M. The ratio of these heating rates gives a result that is consistent with a general comparison between laminar and turbulent flow heating rates in that there is approximately an order of magnitude difference between the heat transfer rates.

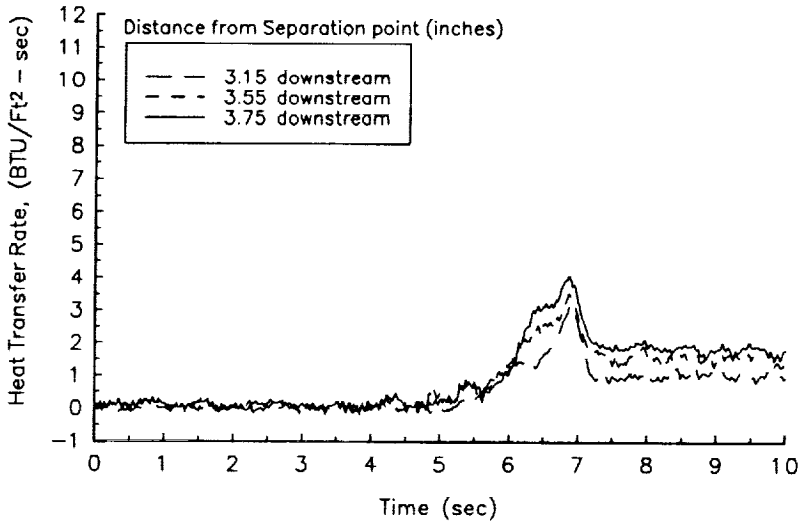

Figure 12. Heating Rate Near Separation: 30° Ramp, Re_b = 4.33 M

Figure 13. Schlieren photograph of a typical "laminar-type" interaction: Re_b = 4.33 M

The self-consistency of these results validates the steady-state character of the temperature response within the shock-boundary layer region. It is still curious, however, that this interacting flowfield does not exhibit any significant or dynamic fluctuations in temperature. This would seem to indicate that steady-state heat transfer analysis should be sufficient for basic configuration design considerations.

CONCLUSIONS

These data show some unsteadiness in temperature response at both the flow separation and reattachment locations, however, the RMS values are of insignificant magnitude. Comparison shows the ratio of these RMS values to the freestream temperature fluctuation levels to be of the order unity. The magnitude of these fluctuations are on the order of 0.5° F in the vicinity of the separation point and approximately 1.0° F in the vicinity of the reattachment point. The lack of any significant temperature fluctuations near the separation point is curious as the pressure response at the separation point indicates a dynamic environment oscillating at frequencies in the range of 300 to 400 Hz[10] with RMS pressure fluctuation levels on the order of 10 times the freestream fluctuation levels. More surprising, however, is the lack of any dynamic temperature trends within the vicinity if the reattachment point. The pressure data indicate significant levels of flowfield unsteadiness. This unsteadiness should appear in the vicinity of the reattachment point. The apparent lack of any temperature fluctuations at both the separation and reattachment locations suggests the flowfield environment is not subject to dynamic temperature effects. The heat transfer rates are steady-state.

ACKNOWLEDGEMENT

The author is deeply indebted to Norm Skaggs and the Air Force Flight Dynamics Directorate for their efforts in providing test time and resources to The Ohio State University through a Cooperative Testing Agreement. This work was supported by the Hypersonic Research and Training Grant administered through NASA and was greatly enhanced by the Air Force Flight Dynamics Directorate at Wright-Patterson AFB.

REFERENCES

1. Dolling, D.S. and Dussauge, J.P., "Fluctuating Wall-Pressure Measurements," Published as Chapter 8 in the Agardograph "A Survey of Measurements and Measuring Techniques in Rapidly Distorted Compressible Turbulent Boundary Layers," Spring 1988.

2. Owen, F.K., "Measurements of Hypersonic Flowfields," AGARD-FDP-VKI Special Course, Aerothermodynamics of Hypersonic Vehicles, 30 May to 3 June 1988.

3. Neumann, R.D., "Aerothermodynamic Instrumentation," AFWAL Technical Paper, WPAFB, May 1989.

4. Miller, C.G. , "Comparison of Thin-Film Resistance Heat-Transfer Gages With Thin-Skin Transient Calorimeter Gages in Conventional Hypersonic Wind Tunnels," NASA TM 83197, 1981.

5. Flanagan, M.J., "Operation and Design Considerations for Unsteady Data Acquisition with PC-Based Systems in High Reynolds Number Flowfields." AIAA Paper 92-0204. Presented at the 30th Aerospace Sciences Meeting, Jan 92.

6. Burke, G.L., "The Effects of Conduction Heat Transfer on the Temperature Distribution of High Speed Vehicles," AFFDL-TM-73-90-FXG, May 1973.

7. Beck, J.V. and TU, J.S., "IHCP2D: Computer Program for Solutions of General Two-Dimensional Inverse Heat Conduction Problems," AFWAL-TR-88-3111, March 1989. Distribution Restricted.

8. Blackman, R.B. and Tukey, J.W., *The Measurement of Power Spectra*, Dover Publications Inc, NY.

9. Marple, S.L., *Digital Spectral Analysis with Applications*, Prentice Hall Signal Process Series, Prentice-Hall Inc, 1987.

10. Flanagan, M.J. and Hayes, J.S., "Pressure and Temperature Fluctuations in an Axisymmetric Flowfield Due to Shock-Boundary Layer Interactions at High Reynolds Number at Mach 6." AIAA Paper 91-3321.